Effects of the surface structure and cluster bombardment on the self-sputtering of molybdenum

2003 J. Phys.: Condens. Matter 15 5845

(http://iopscience.iop.org/0953-8984/15/34/314)

INSTITUTE OF PHYSICS PUBLISHING JOURNAL OF PHYSICS: CONDENSED MATTER

J. Phys.: Condens. Matter **15** (2003) 5845–5855 PII: S0953-8984(03)61777-7

Effects of the surface structure and cluster bombardment on the self-sputtering of molybdenum

E Salonen[1], **T Järvi, K Nordlund and J Keinonen**

Accelerator Laboratory, University of Helsinki, PO Box 43, FIN-00014, Finland

E-mail: msalonen@acclab.helsinki.fi

Received 25 March 2003
Published 15 August 2003
Online at stacks.iop.org/JPhysCM/15/5845

Abstract

The understanding of different features of the sputtering of materials lies in understanding the factors contributing to the emission of atoms from a regular crystal structure at the surface. Although the sputtering of fcc crystals has received much attention, the database on bcc materials is still scarce. We use molecular dynamics simulations to study the self-sputtering of the (100), (110), (111) and (112) surfaces of molybdenum. Single atoms as well as Mo_2 and Mo_4 clusters are used as the irradiation projectiles, in the cluster energy range of 0.125–4 keV. Contrary to the usual assumption, enhanced (nonlinear) sputtering yields are observed for the cluster bombardments at both ends of the energy range studied. The enhancements can be explained with lower threshold energies for sputtering at low energies and with a decreased fraction of channelled projectile atoms in the kiloelectronvolt energy range.

1. Introduction

The erosion of material surfaces by energetic particle bombardment, sputtering, is an intensively studied phenomenon due to its importance in materials modification and characterization. Over the years analytical models for sputtering have been developed, compared to experiments, and refined [1–6]. These models describe the sputtering process as the escape of atoms from a structureless medium with a certain surface potential, surface binding energy, which the atoms must overcome to escape to the vacuum. The results of calculations are then assumed to describe the sputtering of polycrystalline materials, which are composed of textures of crystals with different orientations. However, since different polycrystalline material samples have different crystal textures, the sputtering yields measured for these types of material are known to show a wide scatter [7]. The fundamental understanding of different features of the sputtering process, namely sputtering yields and angular, mass and

[1] Author to whom any correspondence should be addressed.

energy distributions of the ejected particles, requires the understanding of the sputtering of differently oriented crystals of which the studied materials are composed.

The basic understanding of the sputtering of single-crystalline materials [8–11] can be summarized with three main conclusions.

(1) At low energies (below a few hundred electronvolts) the sputtering yields and the threshold energies for sputtering are mainly determined by the surface atom binding energies and simple knock-on sputtering mechanisms, which can be deduced from energy and momentum conservation in collision events.
(2) At energies of a few kiloelectronvolts and higher the 'transparency' of the crystal decreases the sputtering yields, compared to a structureless medium of the same atomic density, due to the channelling of the impinging ions. As the sputtering yields are proportional to the nuclear energy deposited in the surface layers, the channelling of ions reduces the amount of energy available for the ejection of atoms from the surface.
(3) Emission of atoms occurs preferentially in the directions of close-packed rows of atoms. This effect is universally observed in metals, semiconductors and insulators, and over several orders of magnitude in the primary ion energy.

Based on experimental results and theoretical considerations, several sputtering mechanisms underlying the emission of atoms from crystalline materials have been proposed and investigated [12–18]. However, most of the studies of the sputtering of single-crystalline materials in the literature have focused on fcc crystals (see for example the reviews in [8–11]). For bcc materials, which have important applications as radiation resistant materials, e.g. in thermonuclear fusion devices [19], the database is surprisingly scarce.

In order to contribute to the understanding of the sputtering of bcc single-crystalline materials, we have employed classical molecular dynamics (MD) simulations to study the self-sputtering of several crystal surfaces of Mo by single atoms, as well as dimers and tetramers. In the case of Mo_2 and Mo_4 bombardments the main goal of the present work is to investigate the effect of a simultaneous impact of a few projectile atoms in a small surface region. To our knowledge, this type of systematic study on cluster bombardment of different crystal surfaces has not yet been carried out either experimentally or by computer simulations.

2. Simulation method

Our simulation method of ion irradiation of surfaces has been described in detail elsewhere [20–22] and hence we will outline here only the central features of the current study. We first present the force model employed in the modelling and then briefly describe the procedure used for the sputtering simulations.

2.1. Modification and testing of the Mo potential

For the modelling of the interatomic forces between Mo atoms we employed a modification of the Finnis–Sinclair potential [23] by Ackland and Thetford [24]. At short interatomic distances the original potential was smoothly joined to the repulsive Ziegler–Biersack–Littmark potential [25] to realistically model the strong repulsive forces at short ranges. Before carrying out the ion irradiation simulations, several tests were done in order to determine the properties of the modified potential in describing energetic collisions in the Mo bulk structure and at surfaces. The results of the tests, as well as experimental reference values, are summarized in table 1.

Table 1. Test values for the threshold displacement energies $E_d[hkl]$, melting temperature T_{melt} and surface binding energies $U_s(hkl)$ given by the modified Finnis–Sinclair potential. The obtained values are compared to experimental values [26, 34].

	Present work	Experiment
$E_d[100]$ (eV)	33	35^{+1}_{-2} [a]
$E_d[110]$	60	>70[a]
$E_d[111]$	47	45 ± 3[a]
T_{melt} (K)	3000 ± 50	2896[b]
$U_s(100)$ (eV)	7.60	
$U_s(110)$	8.21	
$U_s(111)$	6.73	
$U_s(112)$	7.35	

[a] Reference [26].
[b] Reference [34].

We first determined the threshold displacement energies in the low index directions [100], [110] and [111] with recoil simulations in the Mo bulk structure. Events leading to stable displacement configurations were determined and by gradually lowering the recoil energy the threshold energy for each direction could be found. The minimum displacement energy, 33 ± 1 eV, was determined in the [100] direction. This value is in excellent agreement with the experimental value determined by Maury *et al* [26] from electron irradiation experiments, where the minimum displacement energy of (35^{+1}_{-2}) eV was found in the same direction. The agreement with the other two experimental threshold displacement energies is also good (see table 1).

The melting point of the potential, which is known to affect processes where the formation of dense collision cascades play a role [27, 28], was obtained from simulations of coexisting liquid and solid phases [29]. Although we did not expect any significant spike effects for Mo_1 irradiation in the energy range used in this study (0.125–4 keV), it is known that cluster irradiation can give rise to nonlinear collision cascades and efficient heat spike formation, resulting in enhanced sputtering yields [30].

The surface binding energies $U_s(hkl)$ were calculated by comparing the energy of a pristine, relaxed surface, characterized by the Miller indices (hkl), and the energy of the same surface with one surface atom removed [31]. The magnitudes of the binding energies for different surfaces, ranging from 6.7 to 8.2 eV, were found to have the order $U_s(110) > U_s(100) > U_s(112) > U_s(111)$.

Finally, it should be noted that the clean Mo(100) surface is known to exhibit intricate surface reconstructions at low temperatures [32, 33]. These phase transitions are not reproduced by the potential we have used. However, this does not affect the conclusions of the present work as our irradiation simulations are carried out at 300 K, where no complex surface reconstructions have been observed.

2.2. Irradiation simulations

Mo_n clusters ($n = 1, 2, 4$) were used as the irradiation projectiles, with the total cluster energies E_{cl} ranging between 0.125 and 4 keV. The clusters were assigned random impact points within a unit area on the target surface. The dimers and tetramers were also rotated with random Euler angles in order to obtain arbitrary spatial orientations. The direction of the cluster centre-of-mass velocity was defined by a selected off-normal impact angle θ (either 0° or 20°) and a random twist angle ϕ in the surface plane.

The (100), (110), (111) and (112) surfaces of Mo were used as the irradiation targets. Bulk structures, with periodic boundary conditions, were first equilibrated at 300 K using the temperature and pressure scaling algorithms by Berendsen *et al* [35]. The z-direction was aligned with the normal of the surface plane chosen as the irradiation target. Periodic boundary conditions were then removed in the z-direction, and the target surface was allowed to relaxate for several lattice vibrations. A few bottom layers of the simulation cell were held fixed in order to prevent the formation of another surface. The cubic-shaped target lattice consisted of 3000–80 000 atoms, depending on the cluster energy. Based on our experience on simulating energetic cascades in metals [36–38], these crystal sizes are large enough for a realistic description of the ion impact events.

Temperature scaling [35] was imposed at the cell boundaries in order to model heat conduction into the bulk and to avoid artifacts due to the limited system size (e.g., pressure waves traversing the periodic boundaries). We ensured that no recoiling atoms entered the border region where the temperature scaling was imposed. Inelastic energy losses due to electronic stopping [39] were included in the equations of motion of all atoms having a kinetic energy of 5 eV or higher.

The total simulation time was 3–10 ps. We simulated the irradiation events at the low fluence limit, where a perfect target surface was used for each ion impact. For each combination of target crystal, projectile, off-normal angle and ion energy we ran a total of 100–3000 impact simulations (depending on the number of sputtered atoms) in order to have comprehensive statistics.

3. Results

3.1. Single-atom irradiation

The Mo self-sputtering yields by single atoms at normal incidence are shown in figure 1(a). At energies $\leqslant$0.5 keV it is seen that the sputtering yields from the (111) surface are the highest. This is somewhat expected, as the (111) surface has the lowest surface binding energy of only 6.73 eV. The surface with the second lowest binding energy, (112) with $U_s = 7.35$ eV, also shows high sputtering yields. However, at 125 eV the sputtering yield of the (112) surface is comparable to the ones from the surfaces with higher binding energies, namely the (100) and (110) surfaces.

For energies above 0.5 keV the order of the sputtering yields of different surfaces changes. At 4 keV the differences are the most pronounced, the sputtering yields ranging from 1.7 ± 0.1 for the (111) surface to 3.7 ± 0.3 for the (110) surface. This order of the sputtering yields is in agreement with the experimental study of Mo(100) and Mo(110) irradiation by 5 keV Ar^+ ions by Carlston *et al* [40], where it was observed that $Y_{(110)} > Y_{(100)}$. The experiments further showed that the value of the sputtering yield from polycrystalline Mo would be between the ones for (110) and (100) surfaces.

For a point of comparison to our simulation data there exists only one series of Mo self-sputtering experiments in the energy range of 0.1–10 keV by Saidoh and Sone [41]. Our calculated sputtering yields are in good agreement with the experimental sputtering yields at energies below 1 keV, but somewhat higher at $E > 1$ keV, where the average value for the (100), (110), (111) and (112) surfaces is higher by a factor of 1.7–2. However, it should be noted that the experimental yields in [41] seem to be rather low in comparison with Mo sputtering yields measured with other types of impinging ion [7]. For instance, Weijsenfeld *et al* [42] have reported a Mo sputtering yield of about 0.5 by 1 keV Ne ions. The experiments by Saidoh and Sone [41] show roughly the same value for 1 keV Mo ions, although the nuclear stopping power at this energy is over a factor of four higher [25] for Mo ions than for Ne ions.

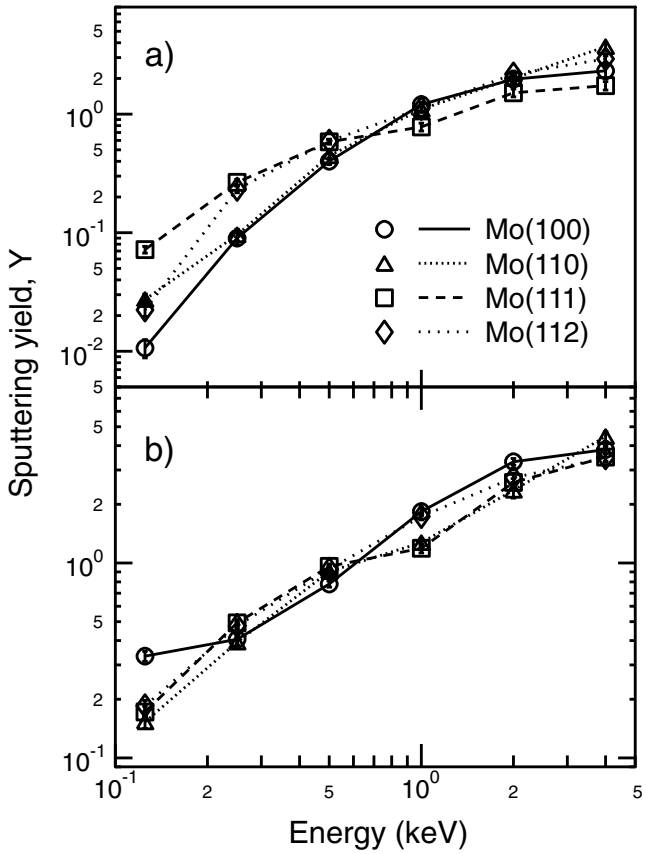

Figure 1. Sputtering yields for Mo(100), (110), (111) and (112) surfaces by Mo_1 bombardment at (a) normal incidence and (b) an off-normal angle of 20°.

In the kiloelectronvolt energy range the channelling of ions is known to have an effect on the sputtering yields [8, 9]. To gain a qualitative understanding of the sputtering yields obtained from the simulations, we follow the model by Onderdelinden [9, 43] assuming that the channelled fraction of the ion beam does not contribute to the sputtering. A rough estimate of the fraction of the ions that channel through the topmost layers can be obtained from the expression

$$f^c_{hkl} = 1 - (E^c_{hkl}/E)^{\frac{1}{2}}; \qquad E \geqslant E^c_{hkl}. \tag{1}$$

E^c_{hkl} is the threshold energy above which channelling becomes efficient for the ion–target combination in question, and is proportional to the unit translation t_{hkl} between atoms in the crystal in the $[hkl]$ direction,

$$E^c_{hkl} \propto (t_{hkl})^3. \tag{2}$$

Following the derivation of E^c_{hkl} in [43], one obtains (neglecting the effect of thermal vibrations) for different Mo surfaces the values $E^c_{111} = 0.6$ keV, $E^c_{100} = 0.9$ keV, $E^c_{110} = 2.5$ keV and $E^c_{112} = 12.8$ keV. Hence, for the (111) and (100) surfaces the effect of channelling on the sputtering yields should be the strongest in the kiloelectronvolt energy range (cf equation (1)). This argumentation is in agreement with the simulations, showing the smallest yields for these surfaces at 4 keV.

Table 2. Depth distributions (in monolayers) of the sputtered atoms from the different surfaces for 4 keV Mo_1 bombardment. The deepest monolayers which contribute to the emitted atom distributions and the average depths of origin of the sputtered atoms are also given (the average depth of the first monolayer atoms is set at 0.0 nm).

		ML				
θ (deg)	Surface (hkl)	1	2	$\geqslant$3	Deepest (ML)	Average depth of origin (nm)
0	(100)	0.77	0.21	0.02	4	0.040
	(110)	0.93	0.06	0.01	4	0.018
	(111)	0.46	0.35	0.19	6	0.066
	(112)	0.63	0.33	0.04	5	0.055
20	(100)	0.79	0.18	0.03	4	0.039
	(110)	0.94	0.05	0.01	3	0.016
	(111)	0.43	0.34	0.23	9	0.078
	(112)	0.64	0.30	0.06	6	0.055

At $\theta = 20^\circ$ there is a noticeable increase in the sputtering yields, compared to $\theta = 0^\circ$, throughout the energy range studied (cf figures 1(a) and (b)). The most interesting observation is that the difference in the sputtering yields of the different surfaces at the lowest energies (125 and 250 eV) is much less pronounced for $\theta = 20^\circ$ than 0°. Except for the (111) surface, the enhancement at $\theta = 20^\circ$ from 0° at 125 eV is about an order of magnitude. It is also worth noting that while for normal incidence the (100) surface shows the lowest sputtering yields at 125 eV, the highest sputtering yield is observed from the same surface at $\theta = 20^\circ$.

It is known [3, 6, 7] that at irradiation energies in the near-threshold regime the sputtering yields decrease very steeply with decreasing energy (several orders of magnitude within a few hundred electronvolts). Furthermore, at least for polycrystalline targets the slope of the sputtering yield as a function of the energy parameter E/E_{th}, where E_{th} is the threshold energy of sputtering, is known to follow a similar scaling law for both light and heavy ion irradiation [44]. This basically means that for two sputtering yield curves in the same low energy range, but with different slopes, a higher threshold energy is expected for the case of the *relatively* steeper slope, falling towards zero more rapidly with decreasing energy.

Comparing the sputtering yield curves in figure 1 for $\theta = 0^\circ$ and 20°, one can clearly see that for the (100), (110) and (112) surfaces the slope changes more strongly at $\theta = 0^\circ$, thus indicating higher threshold energies of sputtering for this impact angle. The differences in the threshold energies of the two angles of incidence then explain why the sputtering yields are higher at $\theta = 20^\circ$. This is quite reasonable, since the threshold energies of sputtering for different ion–surface combinations are known to depend on the angle of incidence [4, 6, 15]. However, in the case of the (111) surface the slopes of the sputtering yield curves of $\theta = 0^\circ$ and 20° are quite similar. This indicates that the threshold energy of sputtering for the (111) surface is less sensitive to a small deviation from the normal angle of incidence than for the other three surfaces.

The depths of origin of the sputtered atoms at 4 keV are given in table 2. It is seen that with decreasing interlayer spacing larger fractions of sputtered atoms originate deeper than the first monolayer. For the case of the smallest interlayer distance, i.e. the (111) surface, less than half of the sputtered atoms come from the first monolayer and about 20% from the third monolayer or deeper. However, in all the cases the average depths of origin are well below 0.1 nm. Comparison between the cases of normal and 20° off-normal incidence shows practically no difference in the depth distributions.

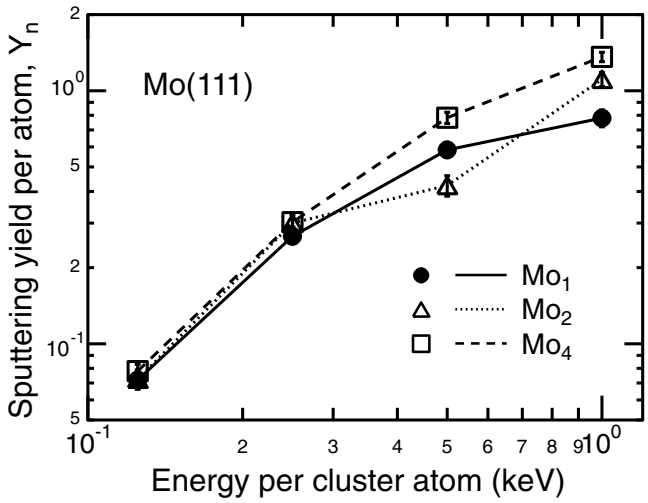

Figure 2. Sputtering yields (per cluster atom) for the Mo(111) surface at normal incidence.

3.2. Mo_2 and Mo_4 irradiation

For the case of small cluster bombardment, it is often assumed that upon impact the cluster of n atoms fragments to separate atoms having roughly equal fractions of the total cluster kinetic energy, $E_n = E_{\mathrm{cl}}/n$. At total energies lower than a few kiloelectronvolts, where no heat spike effects are expected, it is further assumed that the total sputtering yield should be very close to n times the sputtering yield of a single monomer having a kinetic energy of E_n. Hence, we concentrate here on comparing the sputtering yields of dimer and tetramer irradiation per cluster atom, $Y_n = Y/n$, with the case of monomer bombardment at the same values of E_n.

The assumption of linear proportionality between the monomer and small cluster sputtering yields holds extremely well in the case of the bombardment of the (111) surface at the lowest energies (see figure 2). With increasing energy, some fluctuations are observed for the Mo_2 sputtering yields (in comparison with the monomer bombardment) but there is no consistent deviation from the linear proportionality. However, the Mo_4 sputtering yields show a clear trend of enhanced sputtering yields with increasing energy. At $E_n = 1$ keV the ratio of the tetramer to the monomer sputtering yield is about 2.

It was discussed in the case of monomer irradiation (section 3.1) that for the (111) surface and at energies above ∼600 eV, incident ion channelling decreases the sputtering efficiency of the ion beam. For dimer bombardment it can be assumed that the probability of at least one of the dimer atoms having a collision in the topmost monolayers increases. Furthermore, in the case of tetramer bombardment, energetic collisions at the very surface take always place, as the channels are not wide enough to accommodate the whole cluster. Although individual cluster atoms, impacting on random points on the surface, could channel just as efficiently as impinging monomers, the proximity and interactions between the cluster atoms strongly affect the evolution of the impact event. The energetic cluster atoms may affect each other's trajectories after the initial impact on the surface. Even one dechannelling cluster atom perturbs the regular crystal structure of the surface and increases the probability of dechannelling for the other cluster atoms. Hence, the effect of channelling is reduced for cluster bombardment, which then shows as an enhancement in the sputtering yields, when comparing to the single-atom irradiation.

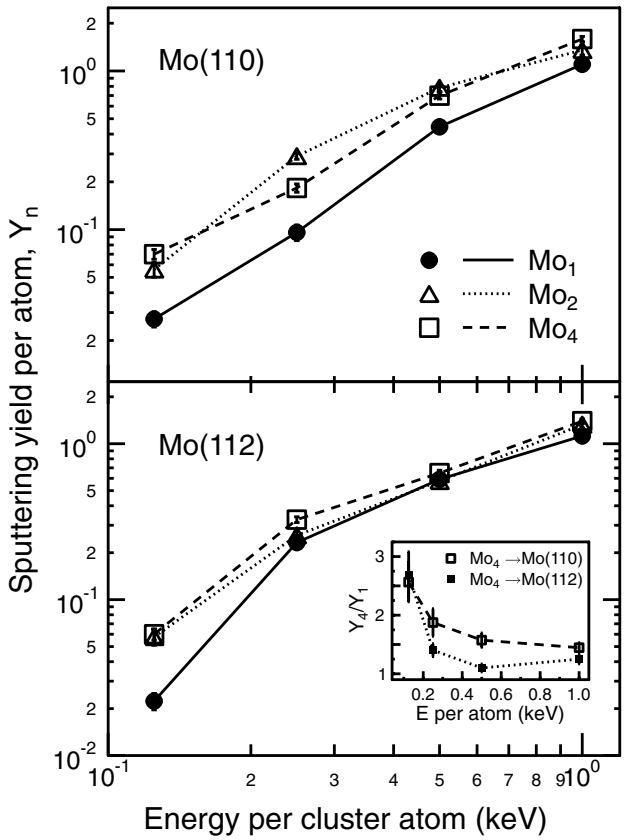

Figure 3. Sputtering yields (per cluster atom) for the Mo(110) (upper panel) and Mo(112) (lower panel) surfaces at normal incidence. The ratios of the sputtering yields by tetramer and monomer bombardments, Y_4/Y_1, for the two surfaces is further illustrated in the inset, showing increasing enhancement with decreasing energy.

For the other three surfaces the results are opposite to those described for the (111) surface above. The linear proportionality for the cluster sputtering yields holds better at the higher energies (although an enhancement of about 25% is seen in the case of tetramer bombardments), whereas strongly enhanced yields are observed at the lower energies. As shown in figure 3 for the (110) and (112) surfaces, the increasing enhancement with decreasing energy clearly points to a lower threshold energy for sputtering. The contribution of reflected projectile atoms to the number of sputtered atoms was of the order of 10^{-3}–10^{-2} and hence cannot be responsible for the enhancements.

The order of the sputtering yields from different surfaces (see table 3) shows the same qualitative trends for the dimer and tetramer bombardments as for the single-atom irradiation. At the lowest energies, however, the differences between the different surfaces are less pronounced for the cluster bombardment. We finally note that the depth distributions of the sputtered species were seen to be similar for all the irradiation projectiles at all energies.

4. Discussion and conclusions

As seen from the results of single-atom irradiation, a simple consideration on the surface binding energies is not sufficient to explain the order of the sputtering yields of the different

Table 3. Sputtering yields (eroded atoms per cluster atom) for the Mo_2 and Mo_4 bombardment.

Ion	E_n (keV)	(100)	(110)	(111)	(112)
Mo_2	0.125	0.04 ± 0.01	0.06 ± 0.01	0.07 ± 0.01	0.06 ± 0.01
	0.25	0.25 ± 0.01	0.29 ± 0.01	0.30 ± 0.01	0.27 ± 0.01
	0.5	0.65 ± 0.03	0.78 ± 0.04	0.42 ± 0.04	0.58 ± 0.03
	1	1.47 ± 0.06	1.36 ± 0.09	1.11 ± 0.07	1.33 ± 0.06
	2	2.0 ± 0.2	2.9 ± 0.1	1.4 ± 0.1	1.8 ± 0.1
Mo_4	0.125	0.06 ± 0.01	0.07 ± 0.01	0.08 ± 0.01	0.06 ± 0.01
	0.25	0.14 ± 0.02	0.18 ± 0.01	0.30 ± 0.02	0.33 ± 0.01
	0.5	0.75 ± 0.03	0.70 ± 0.03	0.78 ± 0.04	0.65 ± 0.03
	1	1.60 ± 0.05	1.59 ± 0.06	1.36 ± 0.06	1.40 ± 0.05

surfaces at near-threshold energies. Whereas the highest sputtering yields for normal incidence are indeed observed for the surface with the lowest value of U_s, namely the (111) surface, the order of the sputtering yields of the other surfaces does not follow the order of the surface binding energies. Moreover, for an off-normal angle of incidence the situation becomes even more complicated: the highest sputtering yields are observed for the (100) surface, which has the second highest value of U_s.

As follows from the theoretical consideration of the near-threshold knock-on sputtering mechanisms by Yamamura and Bohdansky [4], the threshold energies for the different mechanisms are highly dependent on the angle of impact. While the authors considered sputtering from a *random* structure on the basis of the conservations of energy and momentum, it is possible that the regularities of the different crystal structures impose restrictions on one or several of the ejection mechanisms. Two explanations for the decreased threshold energies of sputtering at off-normal angles are then possible:

(1) the sputtering mechanisms for the case of normal incidence become more efficient, as part of the momentum brought into the topmost atom layers by the impinging ion is more efficiently directed toward the surface, and
(2) new collisional pathways leading to atom emission become available. Unfortunately, there is currently no comprehensive theoretical study of the different knock-on sputtering mechanisms from the bcc crystal surfaces which could be used to determine the relative importance of these two factors.

In the case of cluster irradiation, the regularity of the crystal structure at the surface is strongly distorted. It is no longer obvious that only some selected types of collision event could lead to sputtering. Rather, the deposition of a few energetic atoms in a small surface region, as well as any effects due to the random orientation of the impinging cluster, give the sputtering events a pronounced stochastic contribution. It is interesting to note that in a previous study of W(100) irradiation by W clusters [22], no enhancement in the sputtering yields was observed at low energies. However, the lowest energy used in that study was 0.3 keV/atom, which is still quite far from the near-threshold energy regime of W sputtering.

There still remains the question why the enhancement due to cluster bombardment was not observed for the (111) surface at the low energies. We recall that the Mo(111) surface is the one with the most close-packed planes and the lowest surface binding energy of all the surfaces considered here (cf section 2.1). As discussed by Lehmann and Sigmund [13], at near-threshold energies a surface atom has the best probability to be emitted from the surface if it receives energy from a nearest-neighbour head-on collision. This argumentation is also corroborated by the MD simulations by Garrison and co-workers [16–18]. Furthermore, in the

case of the (111) surface the nearest neighbours are aligned in rows perpendicular to the surface plane, which is also the preferential direction of sputtered atom emission from bcc crystals, as known from experiments [10, 11]. Perpendicular emission from a flat surface is the most efficient one for sputtering, as the ability of an atom to escape the surface potential depends on its velocity in the direction of the surface normal [8]. These considerations imply that for the (111) surface the knock-on sputtering mechanisms in single-atom irradiation are already quite efficient. Hence, it could be that the introduction of several cluster atoms simultaneously at the crystal surface does not significantly enhance the efficiency of the collisions events leading to sputtering.

To summarize, we have studied the sputtering of single-crystalline Mo surfaces by Mo_n ($n = 1, 2, 4$) projectiles in the total energy range of 0.125–4 keV. For Mo_1 bombardment the differences in the sputtering yields of the different surfaces cannot be fully explained by a simple consideration of the surface binding energies. At kiloelectronvolt energies the channelling of the impinging ions also has a noticeable effect on the sputtering yields. In the case of cluster bombardment nonlinearities in the sputtering yields are observed at both ends of the energy range considered. At low ($\leqslant$1 keV) energies, enhanced yields by cluster bombardment are observed for the (100), (110) and (112) surfaces due to decreased threshold energies for sputtering. The (111) surface, on the other hand, shows linear yields at low energies, whereas in the kiloelectronvolt energy range enhanced sputtering yields result from decreased fractions of channelled projectile atoms.

Acknowledgments

The research was supported by TEKES under the FFUSION2 programme, and the Academy of Finland under project No 48751. Grants of computer time from the Centre for Scientific Computing in Espoo, Finland are gratefully acknowledged.

References

[1] Sigmund P 1969 *Phys. Rev.* **184** 383
[2] Sigmund P 1981 *Sputtering by Particle Bombardment I* (*Springer Topics in Applied Physics vol 47*) ed R Behrisch (Berlin: Springer) ch 2, pp 9–71
[3] Bohdansky J 1984 *Nucl. Instrum. Methods* B **2** 587
[4] Yamamura Y and Bohdansky J 1985 *Vacuum* **35** 561
[5] Sigmund P 1987 *Nucl. Instrum. Methods Phys. Res.* B **27** 1
[6] García-Rosales C, Eckstein W and Roth J 1994 *J. Nucl. Mater.* **218** 8
[7] Andersen H H and Bay H L 1981 *Sputtering by Particle Bombardment I* (*Springer Topics in Applied Physics vol 47*) ed R Behrisch (Berlin: Springer) ch 4, pp 145–218
[8] Robinson M T 1981 *Sputtering by Particle Bombardment I* (*Springer Topics in Applied Physics vol 47*) ed R Behrisch (Berlin: Springer) ch 3, pp 73–144
[9] Roosendaal H E 1981 *Sputtering by Particle Bombardment I* (*Springer Topics in Applied Physics vol 47*) ed R Behrisch (Berlin: Springer) ch 5, pp 219–56
[10] Hofer W O 1991 *Sputtering by Particle Bombardment III* (*Springer Topics in Applied Physics vol 64*) ed R Behrisch (Berlin: Springer) ch 2, pp 15–90
[11] Gnaser H 1999 *Low-Energy Ion Irradiation of Solid Surfaces* (Berlin: Springer) ch 2
[12] Silsbee R H 1957 *J. Appl. Phys.* **28** 1246
[13] Lehmann C and Sigmund P 1966 *Phys. Status Solidi* **16** 507
[14] Yamamura Y and Takeuchi W 1987 *Nucl. Instrum. Methods Phys. Res.* B **29** 461
[15] Eckstein W, García-Rosales C, Roth J and László J 1993 *Nucl. Instrum. Methods Phys. Res.* B **83** 95
[16] Sanders D E, Prasad K B S, Burnham J S and Garrison B J 1994 *Phys. Rev.* B **50** 5358
[17] Rosencrance S W, Burnham J S, Sanders D E, He C, Garrison B J, Winograd N, Postawa Z and de Pristo A E 1995 *Phys. Rev.* B **52** 6006

[18] Rosencrance S W, Winograd N, Garrison B J and Postawa Z 1996 *Phys. Rev.* B **53** 2378
[19] Federici G *et al* 2001 *Nucl. Fusion* **41** 1967
[20] Nordlund K 1995 *Comput. Mater. Sci.* **3** 448
[21] Nordlund K, Ghaly M, Averback R S, Caturla M, Diaz de la Rubia T and Tarus J 1998 *Phys. Rev.* B **57** 7556
[22] Salonen E, Nordlund K, Keinonen J and Wu C H 2002 *J. Nucl. Mater.* **305** 60
[23] Finnis M W and Sinclair J E 1984 *Phil. Mag.* A **50** 45
[24] Ackland G J and Thetford R 1987 *Phil. Mag.* A **56** 15
[25] Ziegler J F, Biersack J P and Littmark U 1985 *The Stopping and Range of Ions in Matter* (New York: Pergamon)
[26] Maury F, Vajda P, Biget M, Lucasson A and Lucasson P 1975 *Radiat. Eff.* **25** 175
[27] Colla T J and Urbassek H M 2000 *Nucl. Instrum. Methods Phys. Res.* B **164/165** 687
[28] Nordlund K, Henriksson K O E and Keinonen J 2001 *Appl. Phys. Lett.* **79** 3624
[29] Morris J R, Wang C Z, Ho K M and Chan C T 1994 *Phys. Rev.* B **49** 3109
[30] Andersen H H 1993 *K. Danske Vidensk. Selsk. Mat.-Fys. Meddr.* **43** 127
[31] Gades H and Urbassek H M 1992 *Nucl. Instrum. Methods Phys. Res.* B **69** 232
[32] Felter T E, Barker R A and Estrup P J 1977 *Phys. Rev. Lett.* **38** 1138
[33] Daley R S, Felter T E, Hildner M L and Estrup P J 1993 *Phys. Rev. Lett.* **70** 1295
[34] Lide D R (ed) 1995 *CRC Handbook of Chemistry and Physics* 76th edn (Boca Raton, FL: Chemical Rubber Company Press)
[35] Berendsen H J C, Postma J P M, van Gunsteren W F, DiNola A and Haak J R 1984 *J. Chem. Phys.* **81** 3684
[36] Ghaly M, Nordlund K and Averback R S 1999 *Phil. Mag.* A **79** 795
[37] Zhong Y, Nordlund K, Ghaly M and Averback R S 1998 *Phys. Rev.* B **58** 2361 (brief reports)
[38] Nordlund K, Keinonen J, Ghaly M and Averback R S 1999 *Nature* **398** 49
[39] Ziegler J F 1998 SRIM-98 computer code, private communication
[40] Carlston C E, Magnusson G D, Comeaux A and Mahadevan P 1965 *Phys. Rev.* **138** 759
[41] Saidoh M and Sone K 1983 *Japan. J. Appl. Phys.* **22** 1361
[42] Weijsenfeld C H, Hoogendoorn A and Koedam M 1961 *Physica* **27** 763
[43] Onderdelinden D 1968 *Can. J. Phys.* **46** 739
[44] Bohdansky J, Roth J and Bay H L 1980 *J. Appl. Phys.* **51** 2861